Doctor of Philosophy

Study on treatment effect of BST204 in chemotherapy-induced cachexia model for new therapeutic strategies in cachexia

The Graduate School

of the University of Ulsan

Department of Medicine

Ho-jin Kim

Study on treatment effect of BST204 in chemotherapy-induced cachexia model for new therapeutic strategies in cachexia

Supervisor: Jeong Kon Kim

A Dissertation

Submitted to
the Graduate School of the University of Ulsan
In partial Fulfillment of the Requirements
for the Degree of

Doctor of Philosophy in Medical Bioscience

By

Ho-jin Kim

Department of Medicine

Ulsan, Korea

August 2021

Study on treatment effect of BST204 in chemotherapy-induced cachexia model for new therapeutic strategies in cachexia

This certifies that the dissertation of Ho-jin Kim is approved.

Committee chairman: Dr. Dong-Cheol Woo

Committee member: Dr. Hyun Ju Yoo

Committee member: Dr. Kyung Won Kim

Committee member: Dr. Gyunggoo Cho

Committee member: Dr. Jeong Kon Kim

Department of Medicine

Ulsan, Korea

August 2021

Contents

CONTENTS OF TABLES AND FIGURES

ABSTRACT

Chemotherapy is a major etiology of cachexia, and ginseng have various anti-cachetic and health-promoting effects such as inhibiting inflammation and promoting energy production. BST204 is ginseng purified dry extract containing multiple ginsenosides that can reduce chemotherapy-related fatigue and toxicity.

To investigate the effects of BST204 on the alleviation of chemotherapy-induced cachexia using a multimodal approach.

In a CT26 mouse syngeneic colon cancer model, cachexia was predominantly induced by chemotherapy with 5-fluorouracil (5-FU) rather than tumor growth. BST204 at doses of 100 or 200 mg/kg was administered to 5-FU-treated mice.

BST204 significantly mitigated the decrease in tumor-excluded body weight (change in 5-FU group and BST204 groups: -13% vs. -6% on day 7; -30% vs. -20% on day 11), muscle volume (-19% vs. -11%), and fat volume (-91% vs. -56%). The anti-cachetic effect of BST204 was histologically demonstrated by an improved balance between muscle regeneration and degeneration and a decrease in muscle cross-sectional area reduction.

Chemotherapy-induced cachexia was biochemically and metabolically characterized by activated inflammation, enhanced oxidative stress, upregulated protein degradation, downregulated protein stabilization, reduced glucose-mediated energy production, and deactivated glucose-mediated biosynthesis. These adverse effects were significantly impacted by BST204 treatment. Overall, our multimodal study demonstrated that BST204 could effectively alleviate chemotherapy-induced cachexia.

Keywords: Chemotherapy-induced Cachexia, BST204, Multimodal study

ABBREVIATION

3PG, 3-phosphoglycerate

5-FU, 5-Fluorouracil

6PG, 6-phosphogluconate

AMP, Adenosine monophosphate

ATP, Adenosine triphosphate

BW, body weight

CIT/ISO CIT, Citrate/Iso citrate

CSA, cross-sectional area

FBP, Fructose-1,6-bisphosphate

FUM, Fumarate

GLU, glucose

G6P/F6P, glucose-6-phosphate/fructose-6-phosphate

IL-6, interleukin-6

LAC, Lactate

LC-MS/MS, liquid chromatography-tandem mass spectrometry

MAL, Malate

Met-SO, methionine sulfoxide

MRI, magnetic resonance imaging

PEP, Phosphoenolpyruvate

PYR, Pyruvate

R5P, Ribulose-5-phosphate

R15BP, Ribose-1,5-bisphosphate

S7P, Sedoheptulose-7-phosphate

SUC, Succinate

t4-OH-Pro, 4-hydroxyproline

TCA cycle, tricarboxylic acid cycle

I. INTRODUCTION

Cancer cachexia, a complex metabolic syndrome characterized by the severe loss of body weight (BW), which deteriorates the quality of life of cancer patients. In addition to tumor growth, the adverse effects of chemotherapy are a major etiologic factor in cachexia, and could trigger oxidative stress, inflammation, ubiquitin-dependent catabolism, and nitrogen imbalance [1]. These unfavorable responses rather than the tumor growth itself may have a stronger effect on cachexia development. Accordingly, various treatment strategies have been developed to alleviate cancer cachexia [2].

Ginseng is an important natural product for use in the supportive therapy of cancer patients [3]. BST204 is Ginseng purified dry extract that suppresses chemotherapy-related fatigue and toxicity [4]. High concentrations of ginsenosides, the major pharmacological components of ginseng, particularly Rh_2 (7.1%) and Rg_3 (12.1%) in BST204 can effectively reduce inflammatory activity and nitric oxide production [5]. Other components (e.g., Rg2 and Rg5) also inhibit inflammation and oxidative stress and prevent muscle insulin resistance [6-9]. Therefore, it is important to validate BST204 treatment effects for chemotherapy-induced cachexia.

While analyzing multi-component agents such as BST204, a multimodal approach is required to understand their pharmacological modes of action. In this study, the morphological severity of cachexia was estimated using tumor-excluded BW, and the muscle and fat volumes were separately measured by magnetic resonance imaging (MRI). Then, the changes in weight and volumetric indices were pathophysiologically interpreted using histological, biochemical, and metabolomic parameters. Finally, based on the results, we evaluated the effect of chemotherapy on the development of cachexia and the anti-cachexic mechanism of BST204.

. MATERIALS AND METHODS

1. Study design

Detailed information on study design is presented in Figure 1. We generated a cachexia model by administering 5-fluorouracil (5-FU) to CT26 colon cancer mice based on the following rationales: (a) a CT26 syngeneic colon cancer model allows easy establishment and monitoring of cachexia [10]; (b) cachexia degree may vary according to clinically used combination regimens for colon cancer [1] such as FOLFOX, FOLFIRI, and FOLFIRINOX [11]; and (c) 5-FU is commonly included in these combination regimens [12] and can consistently induce cachexia [13-16].

Eight-week-old male BALB/c mice were used in this study. Mice were randomized into five groups (n = 10 each): untreated, non-tumor-bearing mice (NTB group); untreated, tumor-bearing mice (TB group); tumor-bearing mice receiving 5-FU (5-FU group); tumor-bearing mice receiving 5-FU and 100-mg/kg BST204 ($BST204_{100}$ group); and tumor-bearing mice receiving 5-FU and 200-mg/kg BST204 ($BST204_{200}$ group).

CT26 murine colon carcinoma cells (1×10^6) resuspended in 100 μL of phosphate-buffered saline were subcutaneously implanted in the right flank of mice.

When tumor volumes reached 100–200 mm^3 (approximately 10 days after tumor cell injection), day 0 was assigned and drug administration started for 5-FU and BST204 groups. BST204 (batch number 31037/H1) was obtained from Green Cross Wellbeing (Seongnam, South Korea), and 5-FU was purchased from Sigma-Aldrich (St. Louis, MO, USA). 5-FU (50 mg/kg) was injected intraperitoneally in 3-day cycles (1^{st} cycle: days 0–2; 2^{nd} cycle: days 6–8), in doses that did not exceed the clinically acceptable [17]. BST204 (100 or 200 mg/kg) was orally administered in 5-day cycles (1^{st} cycle: days 0–4; 2^{nd} cycle: days 6–10). The BST204 doses were determined according to its effects on chemotherapy-related fatigue and toxicity [4].

The endpoint of our study was determined according to IACUC guidelines, which recommend euthanasia with a maximum tumor volume of 1,500 mm^3 and a BW loss of

20%. Therefore, our study period was limited to day 11. At this point, the change in tumor volumes was up to 810%, and significant cachexia was observed.

2. Animals and cell lines

This study was reviewed and approved by the Institutional Animal Care and Use Committee of Asan Medical Institute of Convergence Science and Technology, Seoul, Korea (IACUC number: 2017-01-050). All procedures were performed according to the relevant guidelines of the National Cancer Institute.

All animals were purchased from Orient Bio (Seongnam, Korea). Five mice were housed per individual cage with environmental enrichment. The housing facility was maintained at automatically controlled system with temperature (24 ± 1 °C), humidity (50 ± 10%) and lighting (12-hour light/dark cycle, lights on at 08:00 AM). Food and water were provided ad libitium throughout the experimental period.

Murine CT26 cells (Korean Cell Line Bank, Seoul, Korea) had been cultured in RPMI 1640 supplemented with 10% fetal bovine serum, 100 U/mL penicillin, and 100 μg/mL streptomycin and maintained at 37 °C in a humidified incubator with 5% CO2

3. MRI for measuring muscle and fat volume

The muscle and fat volumes were separately estimated by MRI. MRI was performed on days 0 and 11. MR images were acquired using a 9.4-T system (Varian; Agilent Technologies, Palo Alto, CA, USA). T1-weighted images were acquired using a fast spin echo pulse sequence (TR = 1100 ms, TE = 10.75 ms, average = 1, field of view = 30 × 30 mm, slice thickness = 1 mm, matrix size = 128 × 128). The region of interest was drawn to include all muscle and fat in each mouse, and these parameters were calculated using Image J software (National Institutes of Health, Bethesda, MD, USA).

4. Body and muscle weight

To exclude the effect of increasing tumor weight on the assessment of cachexia severity, we measured the tumor-excluded body weight (BW) rather than the total BW twice a week. The tumor volume (width^2 × length × 0.52) was measured with a digital caliper and converted to tumor weight by assuming a density of 1 g/cm^3 (Figure 2). Then, the tumor-excluded BW was calculated as the difference between total BW and tumor weight.

As an additional parameter, the weight of the tibialis anterior and gastrocnemius muscles was measured immediately following the sacrifice of mice on day 11.

5. Histological analysis

After sacrifice on day 11, the tibialis anterior muscles were removed and fixed in 4% paraformaldehyde overnight. The muscle samples were then embedded into paraffin blocks. Sections (3-μm thickness) were stained with hematoxylin and eosin. Muscle degeneration was assessed according to the number of hyalinized and hypereosinophilic muscle fibers per total fibers (approximately 2500) [18, 19]. Muscle regeneration was assessed according to the number of muscle fibers with central nuclei per total fibers [20]. The cross-sectional area (CSA) of each muscle fiber was analyzed using ImageJ software.

6. Biochemical and metabolomics assay

To obtain information on a molecular level, we assessed the levels of inflammation, oxidative stress, protein degradation, glucose-mediated energy production, and glucose-mediated biosynthesis in the muscle and plasma. Inflammation degree was estimated based on interleukin-6 (IL-6) and histamine concentrations, which are widely used inflammation measurement parameters [4, 21], as well as kynurenine, since tryptophan is converted to kynurenine during

inflammation [22]. Oxidative stress was measured using methionine sulfoxide, produced from free and/or protein-biding methionine by reactive oxygen species [23]. Protein degradation severity was evaluated based on protein-composing and protein-stabilizing amino acids. Specifically, hydroxyproline was used as an indicator of protein stabilization, as it promotes sharp twisting of the collagen triple helix [24]. Glucose-mediated energy production was assessed measuring glycolysis and tricarboxylic acid (TCA) cycle activities. Finally, glucose-mediated biosynthesis was evaluated by the pentose phosphate pathway activity, as it contributes to fatty acid, nucleotide, nucleic acid, and aromatic amino acid synthesis [25].

7. Plasma IL-6 measurement

For plasma samples, whole blood was harvested via cardiac puncture at terminal stage of the experiment and collected in Ethylenediaminetetraacetic acid (EDTA) containing tubes [26]. To collect plasma, centrifuge the blood sample for 15min at 1500g, 4°C and obtain the supernatant (plasma). Plasma interleukin-6 (IL-6) level was measured using the IL-6 Quantikine mouse enzyme-linked immunosorbent assay kit (R&D Systems, Minneapolis, MN, USA) according to the manufacturer's protocol.

8. Targeted metabolomics by LC-MS/MS

For amino acid and bioamine analysis, the gastrocnemius muscle tissue (25–35 mg) was homogenized using TissueLyser (Qiagen, Hilden, Germany) with 500-μL chloroform/methanol (2/1, v/v). The homogenate was incubated at 4 °C for 15 min. An internal standard containing ^{13}C5-glutamine, serotonine-d_4, dopamine-d_4, tryptophan-d_5, and serine-d_3, at final concentrations of 10, 0.4, 0.6, 2, and 6 μM, respectively, was

prepared. The plasma samples (50–100 μL) were combined with 375 μL of chloroform/methanol (1/2, v/v; 375 μL) and mixed with the internal standard. Samples were centrifuged at 14,000 rpm for 15 min, the supernatant was collected, and H_2O and chloroform (125 μL each) were added. Samples were mixed vigorously and centrifuged at 4,000 rpm for 20 min. The aqueous phase was collected after liquid-liquid extraction (LLE), and half of the solution was used for the chemical derivatization of amino acids and bioamines with phenyl isothiocyante. Subsequently, the derivatized amino acids and bioamines were extracted with 5 mM ammonium acetate in methanol and used for liquid chromatography with tandem mass spectrometry (LC-MS/MS) analyses. The remaining aqueous phase after LLE was used for the analysis of energy metabolites: it was dried under vacuum pressure and reconstituted with 40 μL of H_2O/acetonitrile (50/50, v/v) prior to LC-MS/MS.

Amino acids and bioamines were analyzed using an LC-MS/MS instrument equipped with 1290 HPLC (Agilent Technologies, Palo Alto, CA, USA), Qtrap 5500 (AB Sciex, Framingham, MA, USA), and a reverse-phase column (Zorbax Eclipse XDB-C18100 ×2 mm; Agilent Technologies). The sample (3 μL) was injected into the LC-MS/MS system and ionized with a turbo spray ionization source. Mobile phases A and B consisted of 0.2% formic acid in H_2O and in acetonitrile, respectively. The separation gradient was as follows: 0% B for 0.5 min, 0% to 95% B for 5 min, hold at 95% B for 1 min, 95% to 0% B for 0.5 min, then hold at 0% B for 2.5 min. The LC flow rate was 500 μL/min and column temperature was 50 °C. Multiple reaction monitoring was used in the positive ion mode, and the extracted ion chromatogram (EIC) corresponding to the specific transition for each analyte was used for quantitation. The calibration range was generally 1 nM-600 μM, with $R^2 > 0.98$.

For energy metabolites, an LC-MS/MS equipped with 1290 HPLC, Qtrap 5500 and a reverse-phase column (Synergi fusion RP 50 × 2 mm; Phenomenex, Torrance, CA, USA) was used. Mobile phases A and B consisted of 5 mM ammonium acetate in H_2O and in acetonitrile, respectively. The separation gradient was as follows: 0% B for 5 min, 0% to 90% B for 2 min, hold at 90% B for 8 min, 90% to 0% B for 1 min, and then hold at 0%

B for 9 min. The LC flow rate was 70 μL/min except at 7-15 min when it was 140 μL/min, at 23 °C. Multiple reaction monitoring was used in the negative ion mode, and the area under the curve of each EIC was normalized to the internal standard. Data analysis was performed using Analyst 1.5.2 software.

All of the metabolomics data are publicly available at Metabolomics Workbench (study ID: ST001467).

9. Statistical analysis

Statistical analysis was performed using SPSS (SPSS Inc., Chicago, IL, USA). Non-parametric (Mann-Whitney U-test for two-group comparisons and the Friedman test for multiple group comparison) or parametric (Student's t-test for two-group comparisons and ANOVA with post-hoc test for multiple group comparison) tests were selected according to normality test (Kolmogorov-Smirnov) results. $P < 0.05$ indicated statistical significance.

. RESULTS

BST204 attenuated tumor-excluded BW loss in chemotherapy-induced cachexia model

From day 0 to day 11, cachexia was predominantly induced by chemotherapy rather than by tumor growth. 5-FU group presented a rapid decrease in tumor-excluded BW (up to -30% on day 11), with lower results on days 4, 7, and 11 than TB group, which displayed a -1% tumor-excluded BW change on day 11. The weight gain in NTB group resulted in a significantly greater tumor-excluded BW than in TB group on day 11 (5% *vs.* -1%) (Figure 3).

BST204 (200 mg/kg) markedly alleviated chemotherapy-induced cachexia. The decrease in tumor-excluded BW was significantly lower in $BST204_{200}$ group than in 5-FU group on days 7 and 11 (-6% *vs.* -13% on day 7; -20% *vs.* -30% on day 11). Despite the anti-cachexic effect, $BST204_{200}$ group presented significant decrease in tumor-excluded BW during days 7-11. In contrast to $BST204_{200}$ group, $BST204_{100}$ group did not display significant effect.

BST204 treatment reduced muscle and fat loss in chemotherapy-related cachexia model

5-FU group displayed a marked decrease in muscle (-19%) and fat (-91%) volumes during day 0-11 (Figure 4). Although TB group also presented lower muscle (-3%) and fat (-7%) volumes than NTB group (0% and 14%, respectively), muscle and fat losses were more severe following chemotherapy than by tumor growth. $BST204_{200}$ group (-11% for muscle; -56% for fat) presented significantly alleviated chemotherapy-induced cachexia, with a lower degree of muscle and fat loss than 5-FU group. $BST204_{100}$ group showed significant results only for fat loss (-18% for muscle; -71% for fat).

BST204 administration alleviated muscle weight loss in chemotherapy-induced cachexia model

Intergroup comparisons for muscle weight demonstrated both chemotherapy-induced muscle atrophy and an anti-cachexic effect in both BST204 groups (Figure 5). Muscle weight was significantly lower in 5-FU group than in TB group. Although TB group presented a lower gastrocnemius muscle weight than NTB group, muscle atrophy degree was more severe following chemotherapy than tumor growth. Compared with 5-FU group, both BST204 groups presented significantly greater weight of both muscles, thereby demonstrating the anti-cachetic effect.

BST204 increased muscle regeneration activity and decreased muscle degeneration activity in chemotherapy-related cachexia model

Histological analyses provided cell-level evidence of chemotherapy-induced muscle atrophy and the anti-cachexic effect of BST204 (Figure 6).

An imbalance between muscle degeneration and regeneration was the main cause of chemotherapy-induced muscle atrophy. Compared with TB group, 5-FU group had higher muscle degeneration activity and lower muscle regeneration activity. Similar parameters between TB and NTB groups indicated that muscle atrophy was caused predominantly by chemotherapy than by tumor growth.

Compared with 5-FU group, both BST204-treated groups demonstrated higher muscle regeneration activity and lower muscle degeneration activity. Muscle CSA was significantly lower in 5-FU group than in TB group. Although muscle CSAs in TB group were also lower than in NTB group, this reduction was more affected by chemotherapy than by tumor growth. $BST204_{200}$ group had a significantly higher muscle CSA than 5-FU group, whereas $BST204_{100}$ group did not present statistically different results.

BST204 suppressed inflammation and oxidative stress in chemotherapy-induced cachexia model

Inflammation degree was evaluated based on IL-6, histamine, and kynurenine levels [4, 21, 22], and oxidative stress was quantified according to methionine sulfoxide level [23]. Comparisons of inflammation and oxidative stress between groups are summarized in Figure 7, Tables 1 and 2. Higher levels of these parameters in 5-FU group than in TB group indicated chemotherapy-induced upregulation of inflammation and oxidative stress.

Chemotherapy-induced inflammation and oxidative stress were effectively suppressed by BST204 treatment. Compared with 5-FU group, both BST204-treated groups had lower kynurenine and methionine sulfoxide levels in the muscle and/or plasma. Moreover, the levels of these parameters in BST204-treated groups were similar to those in NTB group, indicating alleviation of chemotherapy-induced inflammation and oxidative stress. These parameters did not differ between $BST204_{100}$ and $BST204_{200}$ groups.

BST204 reduced the chemotherapy-induced imbalance of protein degradation and stabilization in chemotherapy-related cachexia model

Protein degradation and stabilization were measured based on the level of protein-composing amino acids and of a protein stabilizer (t4-hydroxyproline [24]), respectively. Intergroup comparisons of protein degradation and stabilization are summarized in Figure 7, Tables 1 and 2. Compared with TB group, 5-FU group had higher levels of protein-composing amino acids in the muscle, including alanine, asparagine, aspartate, histidine, isoleucine, leucine, methionine, phenylalanine, proline, serine, threonine, tryptophan, tyrosine, and valine. This indicated that these amino acids were released from damaged proteins and accumulated in the muscle. 5-FU group had a lower protein stabilizer level in muscles. These results indicate that chemotherapy disrupted the balance between protein degradation and stabilization.

BST204 treatment reduced the chemotherapy-induced imbalance in protein degradation and stabilization as protein-composing amino acid levels were lower and protein stabilizer level was higher in both BST204-treated groups than in 5-FU group. These effects were similar between $BST204_{100}$ and $BST204_{200}$ groups.

BST204 activated glucose-mediated energy production in chemotherapy-induced cachexia model

Glucose-mediated energy production was assessed based on the muscular and plasma levels of glucose, glycolysis intermediates, and TCA cycle intermediates (Figure 8, Tables 3 and 4). Compared with TB group, 5-FU group demonstrated decreased glucose-mediated energy production, indicated by lower levels of glucose, glycolysis intermediates (glucose-6-phosphate, fructose-1,6-bisphosphate, 3-phosphoglycerate, and phosphoenolpyruvate in the muscle and plasma), and TCA cycle intermediates (succinate in the muscle; citrate, succinate, fumarate, and malate in the plasma). Owing to inactivated glucose metabolism, 5-FU group had a lower ATP level and a higher AMP/ATP ratio (a marker of ATP depletion [27]) compared with TB group considering both the muscle and plasma.

BST204 treatment reversed this effect. Compared with 5-FU group, $BST204_{200}$ group had significantly higher glucose, glycolysis intermediate (glucose-6-phosphate, fructose-1,6-bisphosphate, 3-phosphoglycerate, phosphoenolpyruvate, pyruvate, and lactate in the muscle; glucose-6-phosphate and phosphoenolpyruvate in the plasma), and TCA cycle intermediate levels (succinate in the muscle; citrate, succinate, and fumarate in the plasma). Owing to an increased activity of glycolysis and the TCA cycle, $BST204_{200}$ group had higher ATP level and lower AMP/ATP ratio than 5-FU group in the muscles. A smaller number of metabolites returned to their normal values in $BST204_{100}$ group than in $BST204_{200}$ group.

BST204 activated glucose-mediated biosynthesis in chemotherapy-induced cachexia model

Glucose-mediated biosynthesis was evaluated based on the level of pentose

phosphate pathway metabolites [25] (Figure 9, Tables 3 and 4). Compared with TB group, 5-FU group displayed lower plasma levels of pentose phosphate pathway metabolites (6-phosphogluconate, ribulose-5-phosphate, ribose-1,5-bisphosphate, and sedoheptulose-7-phosphate). Compared with 5-FU group, both BST204-treated groups had higher levels of these metabolites, thereby indicating reactivated glucose-mediated biosynthesis.

. DISCUSSION

Tumor progression and chemotherapy are two major causes of cancer cachexia. Although these factors share some common signaling pathways [17], their effects on the development and sustainment of cachexia may be differ according to the time course, anticancer agents, tumor types, and tumor-drug interactions. Recognizing this differences is important for establishing pathophysiology-specific treatment strategies. In comparison with tumor-host interactions, the molecular mechanism of chemotherapy-induced cachexia remains mostly undiscovered. In a related study, Barreto *et al.* reported the effect of chemotherapy alone in cachexia development and observed that cisplatin administration to NTB mice led to severe muscle wasting via upregulated ERK1/2 and p38 MAPK pathways [1]. However, this may not reflect the conditions of cancer-burdened hosts; hence, we observed chemotherapy-induced cachexia in TB mice. In addition to the tumor-excluded BW and muscle/fat volume, various histological, biochemical, and metabolomic parameters indicated that cachexia was caused predominantly by chemotherapy rather than tumor growth.

In our multimodal analysis, 5-FU increased stress levels (i.e., inflammation and oxidative stress) and altered the metabolism (i.e., enhanced protein degradation, inactivated protein stabilization, decreased glucose-mediated energy production, and reduced glucose-mediated biosynthesis). These results suggest that multiple molecular pathways may be closely related to chemotherapy-induced cachexia; therefore multipotential therapeutic agents may be more helpful than those targeting a single pathway for its treatment.

As a multipotential therapeutic, BST204 contains a various ginsenosides including Rh2, Rg3, Rb1, Rc, Rd, Rg1, and F2 [28]. Notably, its high Rh2 and Rg3 concentrations strongly suppress the action of inflammatory mediators, such as prostaglandin E2, cyclooxygenase-2, tumor necrosis factor-α, IL-6, inducible nitric oxide synthase, and nitric oxide [4, 5, 29]. Other ginsenosides are also known to have several health-promoting effects. Representatively, the ginsenosides Rb1 and Rg3 can mitigate dysregulated glucose metabolism by increasing insulin sensitivity through activating AMP-activated protein kinase [30, 31]. Increased glucose uptake,

possibly due to Rb1 and Rg3 in BST204, might be related to the upregulated energy metabolism and biosynthesis of non-essential amino acids, because these amino acids are mainly generated from glycolysis and TCA cycles (reference: book chapter; Metabolism at a glance, 4th ed. J. G. Salway, Wiley Blackwell). In our study, most of the amino acids in the muscles of $BST204_{200}$ group was reduced compared to those in the 5-FU group, because the amino acids were consumed for protein regeneration. However, the reduction in non-essential amino acids, such as alanine and aspartate, was not significant, possibly due to enhanced energy metabolism. Futher, the decreased oxidative stress due to Rh2 in BST204 group may increase the availability of recycled amino acids for protein regeneration. In our study, methionine sulfoxide was significantly increased in the 5-FU group and reduced in $BST204_{200}$ group.

Several studies reported that cancer and chemotherapy-related cachexia induced loss of skeletal muscle and fat mass [1, 32]. Particularly, an imbalance between muscle degeneration and regeneration is the primary mechanism of muscle wasting [33]. In this study, BST204 demonstrated significant anti-cachetic effects. BST204 (200 mg/kg) significantly attenuated the decrease in tumor-excluded BW (from -13% to -6% on day 7 and from -30% to -20% on day 11). The chemotherapy driven muscle and fat losses were reduced from -20% to -11% and from -91% to -56%, respectively. These phenotypic effects may be attributed to restoration of histological and molecular parameters. BST204 strongly suppressed chemotherapy-related inflammation and oxidative stress and significantly restored the altered amino acid and glucose metabolism to normalcy. These modes of therapeutic action improved the balance between muscular degeneration and regeneration and eventually alleviated BW and muscle/fat volume reduction.

A comparison between $BST204_{100}$ and $BST204_{200}$ groups revealed that the anti-cachetic effect of a 200 mg/kg dose was superior to that of 100 mg/kg; tumor-excluded BW restoration was significant only in $BST204_{200}$ group. Moreover, the anti-cachexic effect in $BST204_{200}$ group was variable over time; this group maintained tumor-excluded BW from day 4 to 7 but experienced significant BW loss from day 7 to 11. Therefore, the anti-cachetic effect of BST204 may depend on the burden of the cachexia stage in addition to the therapeutic dose.

These factors should be carefully considered when planning clinical trials.

Increased inflammation and oxidative stress in cancer and chemotherapy-associated cachexia have been reported in a number of studies [34-36]. Futher, glucose metabolic dysfunction related to chemotherapy-induced cachexia has been shown in previous studies [17, 32]. Thus, inflammation, oxidative stress and glucose metabolism, which are the key-biomarkers of chemotherapy-induced cachexia, were investigated in this study. Owing to extreme cachexia in the 5-FU group, we could not obtain a sufficient amount of fat for molecular analysis. We assume that this chemotherapy-induced fat loss was driven by both stress-induced lipolysis and excessive lipid consumption. Lipolysis is accelerated by inflammation via pro-inflammatory cytokines and by oxidative stress via reactive lipid aldehydes [37, 38]. Moreover, the glucose overconsumption under upregulated inflammation and oxidative stress is compensated by using fatty acids in ATP production [39]. Therefore, the reduction in fat loss caused by BST204 treatment appears to be the result of improved energy metabolism.

The use of animal models is vital in preclinical cachexia study. We generated a cachexia model by inoculating CT26 colon cancer cells to BALB/c mice. In comparison with genetically engineered mouse models, the commonly used CT26 syngeneic mouse model is characterized by a rapid onset of tumor growth and cachexia, allowing easier establishment, monitoring, and reproduction [10]. However, in contrast to previous studies [40, 41], our model did not show significant cancer-driven cachexia. We believe that differences in the study periods may be mostly responsible for this inter-study variation. Our study was interrupted at 11 days after the tumors were palpated (approximately 100-200 mm^3) because the tumor volumes reached 1,500 mm^3 or the BW was decreased to 20% of the initial value. In this period, cancer-driven cachexia was not apparent despite significant tumor growth; nonetheless, notable cachexia was induced by chemotherapy. Considering that combination chemotherapy regimens are administered as adjuvant treatments for colon cancer without significant cancer-driven cachexia, our study would be more similar to the clinical conditions than studies with cancer-driven cachexia. Therefore, our results suggest that significant cachexia can occur even before the onset of cancer-driven cachexia, and treatment for chemotherapy-induced cachexia should be considered when planning adjuvant chemotherapy.

This study measured the tumor-excluded BW rather than total BW because the exclusion of tumor volume improves the accuracy in estimating the severity of cachexia. The strength of this approach was demonstrated in the comparison between NTB and TB groups (Figure 10). On day 11, the tumor-excluded BW was significantly lower in the TB group than in the NTB group, although their total BW values were similar.

The results of our biochemical and metabolomic assays may be dependent on tumor growth or shrinkage, in addition to the 5-FU and BST204 treatments, because cancer cells can affect inflammation, oxidative stress, and glucose/nitrogen metabolism. However, the differences in these parameters were greater between the 5-FU and BST204 groups and the TB and 5-FU groups than between the NTB and TB groups, indicating that our molecular analyses were able to demonstrate the effects of 5-FU and BST204 rather than those of only tumor-host interactions.

In present study, the muscle regenerative potential of BST204 was confirmed through histological analysis; however, it is necessary to identify molecular markers of muscle regeneration, such as PAX7, Myogenin, MyoD, and MyHC-embrional/neonatal in the muscle [42]. In addition, further research is needed to confirm the molecular mechanism for the anti-cachectic effect of BST204. For example, it has been reported that muscle atrophy is related to the IL6-mediated JAK/STAT3 pathway in both mouse models and patients with cachexia [43-45]. The anti-inflammatory effect of BST204, especially the inhibition of the plasma IL-6 levels, suggests that BST204 is associated with the IL-6/JAK/STAT3 pathway.

TABLES AND FIGURES

Table 1

	Muscle level				Plasma level			
	TB / NTB	5-FU / TB	$BST204_{100}$ / 5-FU	$BST204_{200}$ / 5-FU	TB / NTB	5-FU / TB	$BST204_{100}$ / 5-FU	$BST204_{200}$ / 5-FU
Inflammation								
Histamine	n.s.	n.s.	n.s.	n.s.	n.s.	↑(1.48)	↓(0.43)	↓(0.63)
IL-6					↑	↑(28.45)	↓(0.74)	↓(0.17)
Kynurenine	n.s.	↑(4.07)	↓(0.30)	↓(0.43)	n.s.	↑(1.68)	n.s.	↓(0.65)
Oxidative stress								
Methionine sulfoxide	n.s.	↑(3.30)	↓(0.39)	↓(0.39)	n.s.	↑(1.74)	↓(0.49)	↓(0.54)
Protein-composing amino acids								
Alanine	n.s.	↑(1.39)	↓(0.77)	n.s.	n.s.	↓ (0.74)	n.s.	↑(1.71)
Arginine	n.s.	n.s.	n.s.	n.s.	↑(1.53)	n.s.	n.s.	n.s.
Asparagine	n.s.	↑(2.06)	↓(0.63)	n.s.	n.s.	n.s.	↓(0.62)	↓(0.70)
Aspartate	n.s.	↑(1.52)	n.s.	n.s.	↑(2.37)	n.s.	n.s.	n.s.
Glutamine	n.s.	n.s.	↓(0.65)	n.s.	↑(1.17)	↓ (0.89)	n.s.	n.s.
Glycine	↓(0.3)	n.s.	n.s.	n.s.	n.s.	↓(0.65)	n.s.	n.s.
Histidine	n.s.	↑(1.51)	↓(0.82)	n.s.	n.s.	n.s.	n.s.	n.s.
Isoleucine	n.s.	↑(2.36)	↓(0.47)	↓(0.60)	n.s.	n.s.	n.s.	n.s.
Leucine	↓(0.75)	↑(2.49)	↓(0.48)	↓(0.67)	n.s.	n.s.	n.s.	↓(0.67)
Methionine	↓(0.60)	↑(2.13)	n.s.	n.s.	n.s.	↓ (0.65)	n.s.	↑(1.18)
Phenylalanine	n.s.	↑(2.37)	↓(0.48)	↓(0.66)	n.s.	↑(1.40)	n.s.	↓(0.66)
Proline	↓(0.66)	↑(1.80)	↓(0.56)	↓(0.80)	n.s.	n.s.	n.s.	n.s.
Serine	↓(0.62)	↑(1.36)	n.s.	n.s.	n.s.	n.s.	n.s.	n.s.
Threonine	n.s.	↑(1.67)	↓(0.79)	↓(0.90)	n.s.	n.s.	↓(0.69)	n.s.
Tryptophan	n.s.	↑(1.26)	n.s.	n.s.	n.s.	n.s.	n.s.	↑(1.32)
Tyrosine	↓(0.42)	↑(1.69)	↓(0.73)	↓(0.86)	↓(0.52)	n.s.	n.s.	n.s.
Valine	n.s.	↑(2.31)	↓(0.47)	↓(0.61)	n.s.	n.s.	n.s.	n.s.
Protein stabilizer								
t4-hydroxyproline	n.s.	↓(0.16)	↑(3.55)	↑(3.76)	n.s.	↓ (0.39)	↑(1.88)	↑(1.72)

Table 1. Intergroup comparison of IL-6 and amino acid metabolite concentrations

↑ indicates significantly higher levels, and ↓ indicates significantly lower levels ($P < 0.05$). The numbers between parentheses represent the relative concentrations between groups. IL-6 concentration was measured in 5 mice from each group, and amino acid metabolites were evaluated in 6 mice from each group. NTB, untreated, non-tumor-bearing mice; TB, untreated, tumor-bearing mice; 5-FU, tumor-bearing mice treated with 5-fluorouracil; $BST204_{100}$, tumor-bearing mice treated with 5-fluorouracil and 100 mg/kg of BST204; $BST204_{200}$, tumor-bearing mice treated with 5-fluorouracil and 200 mg/kg of BST204; n.s., not statistically significant.

Table 2

	Muscle level					Plasma level				
	NTB group	TB group	5-FU group	$BST204_{100}$ group	$BST204_{200}$ group	NTB group	TB group	5-FU group	$BST204_{100}$ group	$BST204_{200}$ group
Amino acids (μM)										
Alanine	28.31	18.42	25.62	19.65	22.77	575.3	449.7	330.7	468.3	566.2
Arginine	1.554	1.846	1.590	1.670	2.167	28.13	43.08	33.62	29.52	30.66
Asparagine	2.944	1.755	3.611	2.289	2.827	88.62	85.70	107.7	66.58	75.83
Aspartate	3.320	1.982	3.012	2.658	3.300	7.525	17.70	15.33	11.26	12.72
Glutamine	57.14	46.84	58.42	38.23	69.26	353.5	418.0	372.2	349.3	427.0
Glycine	122.6	37.34	36.00	35.81	32.16	80.75	94.67	61.42	41.97	61.59
Histamine	0.229	0.237	0.287	0.286	0.343	0.061	0.055	0.081	0.035	0.051
Histidine	5.125	4.040	6.087	4.962	6.140	57.47	51.17	63.94	49.05	50.72
Isoleucine	1.834	1.413	3.333	1.580	2.005	462.5	466.7	447.7	456.2	365.2
Kynurenine	40.00 ($\times10^{-4}$)	48.30 ($\times10^{-4}$)	19.70 ($\times10^{-3}$)	58.30 ($\times10^{-3}$)	85.40 ($\times10^{-4}$)	1.638	1.985	3.344	2.483	2.179
Leucine	3.901	2.945	7.326	3.531	4.904	1082	948.7	1162	1102	782.8
Methionine	85.96	51.80	110.5	79.47	89.38	4160	3835	2499	3055	2959
Methionine sulfoxide	20.84	18.45	60.88	24.02	23.63	975.3	1181	2060	1010	1116
Proline	5.375	3.565	6.423	3.625	5.109	12.82	16.23	14.46	16.07	15.37
Phenylalanine	0.838	0.746	1.765	0.851	1.164	161.8	153.5	212.3	143.1	140.7
Serine	7.652	4.754	6.459	5.987	6.798	83.02	66.32	80.55	71.72	78.74
t4-Hydroxyproline	3.424	2.211	0.352	1.250	1.325	5.938	6.753	2.638	4.962	4.545
Threonine	9.852	5.843	9.735	7.700	8.774	133.3	124.2	159.3	110.4	126.8
Tryptophan	1.304	1.351	1.697	1.479	1.641	166.8	122.0	105.6	129.2	139.9
Tyrosine	3.154	1.325	2.233	1.620	1.923	32.75	16.92	19.45	12.95	13.24
Valine	10.71	7.671	17.75	8.409	10.91	2850	2410	2535	2442	2098
Pro-inflammatory cytokine (pg/ml)										
IL-6						n.d.	34.8	990.0	736.2	168.2

Table 2. Concentration of amino acids and plasma IL-6

NTB, untreated, non-tumor-bearing mice; TB, untreated, tumor-bearing mice; 5-FU, tumor-bearing mice treated with 5-fluorouracil; $BST204_{100}$, tumor-bearing mice treated with 5-fluorouracil and 100 mg/kg of BST204; $BST204_{200}$, tumor-bearing mice treated with 5-fluorouracil and 200 mg/kg of BST204; n.d., not detected.

Table 3

	Muscle level				Plasma level			
	TB / NTB	5-FU / TB	BST204$_{100}$ / 5-FU	BST204$_{200}$ / 5-FU	TB / NTB	5-FU / TB	BST204$_{100}$ / 5-FU	BST204$_{200}$ / 5-FU
Glucose-mediated energy production								
Glucose	n.s.	↓(0.65)	↑(1.63)	↑(1.89)	↓(0.80)	↓(0.65)	↑(1.76)	↑(1.49)
Glycolysis								
Glucose-6-phosphate	n.s.	↓(0.09)	n.s.	↑(4.84)	n.s.	↓(0.47)	↑(1.50)	↑(1.49)
Fructose-1,6-bisphosphate	n.s.	↓(0.08)	n.s.	↑(6.04)	↑(2.10)	↓(0.35)	n.s.	n.s.
3-Phosphoglycerate	n.s.	↓(0.15)	n.s.	↑(3.87)	↑(1.35)	↓(0.56)	n.s.	n.s.
Phosphoenolpyruvate	n.s.	↓(0.13)	n.s.	↑(6.94)	n.s.	↓(0.55)	n.s.	↑(1.26)
Pyruvate	↓(0.77)	n.s.	n.s.	↑(1.55)	n.s.	n.s.	n.s.	n.s.
Lactate	n.s.	n.s.	n.s.	↑(1.49)	n.s.	n.s.	n.s.	n.s.
TCA cycle								
Citrate	n.s.	n.s.	n.s.	n.s.	n.s.	↓(0.16)	↑(3.47)	↑(2.77)
Succinate	n.s.	↓(0.44)	↑(1.94)	↑(1.74)	n.s.	↓(0.24)	n.s.	↑(3.21)
Fumarate	n.s.	n.s.	n.s.	n.s.	↓(0.29)	↓(0.28)	↑(2.73)	↑(2.42)
Malate	n.s.	n.s.	n.s.	n.s.	↓(0.29)	↓(0.50)	n.s.	n.s.
Energy metabolites								
AMP	↓(0.42)	↑(1.59)	n.s.	↓(0.68)	n.s.	n.s.	n.s.	n.s.
ATP	n.s.	↓(0.28)	↑(2.35)	↑(2.39)	↓(0.54)	↓(0.53)	n.s.	n.s.
AMP/ATP	↓(0.22)	↑(6.84)	↓(0.29)	↓(0.26)	n.s.	↑(3.82)	n.s.	n.s.
Glucose-mediated biosynthesis								
Pentose phosphate pathway								
6-Phosphogluconate	n.s.	↓(0.38)	↑(1.83)	↑(2.13)	↑(1.48)	↓(0.36)	↑(2.04)	↑(1.92)
Ribulose-5-phosphate	n.s.	n.s.	n.s.	n.s.	↑(1.44)	↓(0.48)	n.s.	↑(1.27)
Ribose-1,5-bisphosphate	n.s.	n.s.	n.s.	n.s.	↑(1.20)	↓(0.63)	↑(1.47)	↑(1.23)
Sedoheptulose-7-phosphate	n.s.	↓(0.52)	n.s.	↑(1.85)	↑(1.74)	↓(0.30)	↑(1.74)	↑(1.67)

Table 3. Intergroup comparison of glucose metabolite levels

↑ indicates significantly higher levels, and ↓ indicates significantly lower levels ($P < 0.05$). Levels between groups are indicated between parentheses. The concentrations of glucose metabolites were analyzed in 6 mice from each group. NTB, untreated, non-tumor-bearing mice; TB, untreated, tumor-bearing mice; 5-FU, tumor-bearing mice treated with 5-fluorouracil; $BST204_{100}$, tumor-bearing mice treated with 5-fluorouracil and 100 mg/kg of BST204; $BST204_{200}$, tumor-bearing mice treated with 5-fluorouracil and 200 mg/kg of BST204; n.s., not statistically significant.

Table 4

	Muscle level					Plasma level				
	NTB group	TB group	5-FU group	BST204$_{100}$ group	BST204$_{200}$ group	NTB group	TB group	5-FU group	BST204$_{100}$ group	BST204$_{200}$ group
Glucose	119.6	94.24	61.02	99.48	115.4	650.0	521.9	337.3	593.4	502.4
Glycolysis										
Glucose-6-phosphate	30.00	28.57	2.47	8.73	11.95	1.931	2.099	0.988	1.482	1.469
Fructose-1,6-bisphosphate	9.482	9.939	0.775	3.194	4.677	0.211	0.442	0.155	0.268	0.220
3-Phosphoglycerate	3.075	3.460	0.533	1.245	2.062	0.745	1.007	0.564	0.511	0.669
Phosphoenolpyruvate	0.450	0.731	0.094	0.275	0.656	0.383	0.437	0.240	0.227	0.302
Pyruvate	29.19	22.38	17.44	23.26	26.96	81.55	73.07	61.03	63.45	74.18
Lactate	293.7	229.5	183.9	218.5	273.5	747.5	521.9	658.9	654.5	760.2
TCA cycle										
Citrate	8.616	4.201	4.557	4.701	3.984	1247	1147	178.6	619.0	493.9
Succinate	10.33	5.450	2.419	4.696	4.208	11.09	7.331	1.785	4.504	5.730
Fumarate	3.697	2.356	1.892	2.196	2.455	8.929	2.593	0.729	1.994	1.764
Malate	27.01	16.94	12.61	14.86	17.91	85.69	25.11	12.50	16.79	16.49
Energy metabolites										
AMP	0.522	0.219	0.347	0.250	0.236	0.174	0.081	0.155	0.101	0.102
ATP	0.559	0.785	0.218	0.513	0.521	0.109	0.059	0.031	0.039	0.030
AMP/ATP	1.445	0.317	2.171	0.634	0.572	1.715	1.390	5.315	6.298	4.749
Pentose phosphate pathway										
6-Phosphogluconate	0.269	0.276	0.104	0.190	0.221	5.926	8.747	3.152	6.420	6.061
Ribulose-5-phosphate	1.573	1.401	1.699	1.410	1.831	0.704	1.015	0.490	0.545	0.623
Ribose-1,5-bisphosphate	0.017	0.013	0.015	0.013	0.017	0.209	0.252	0.158	0.231	0.193
Sedoheptulose-7-phosphate	0.141	0.140	0.072	0.082	0.133	0.694	1.210	0.369	0.641	0.616

Table 4. Level of glucose metabolites

NTB, untreated, non-tumor-bearing mice; TB, untreated, tumor-bearing mice; 5-FU, tumor-bearing mice treated with 5-fluorouracil; $BST204_{100}$, tumor-bearing mice treated with 5-fluorouracil and 100 mg/kg of BST204; $BST204_{200}$, tumor-bearing mice treated with 5-fluorouracil and 200 mg/kg of BST204; n.d., not detected.

Figure 1

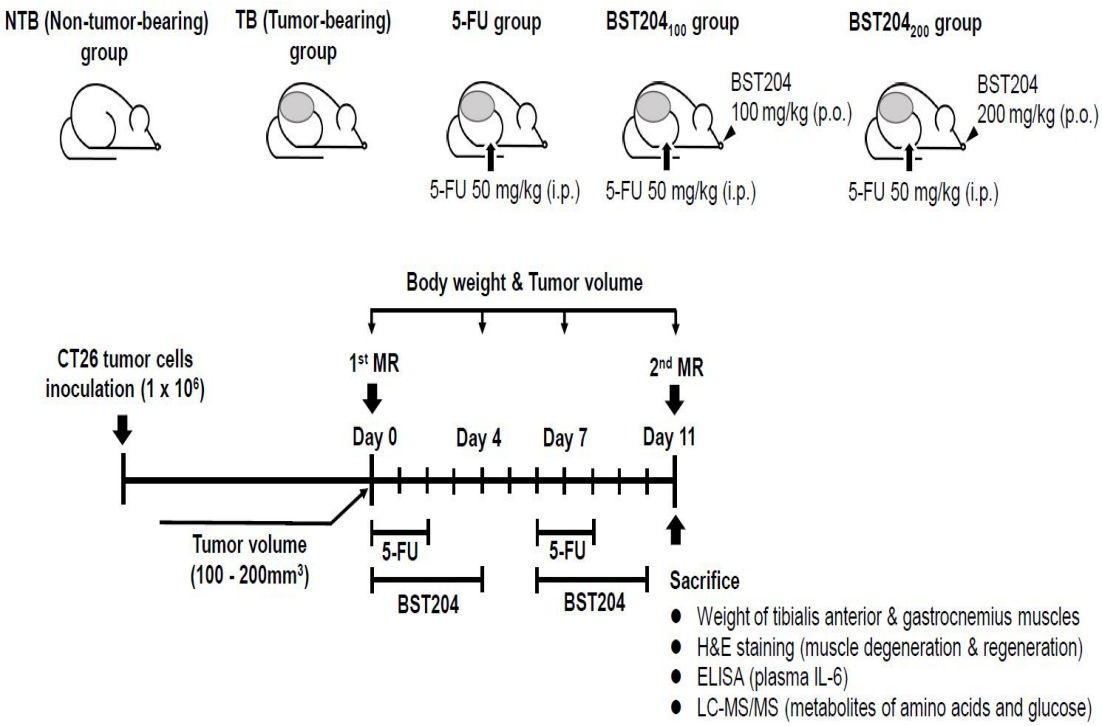

Figure 1. Schematic illustration of the experimental design.

NTB, untreated, non-tumor-bearing mice; TB, untreated, tumor-bearing mice; 5-FU, tumor-bearing mice treated with 5-fluorouracil; $BST204_{100}$, tumor-bearing mice treated with 5-fluorouracil and 100 mg/kg of BST204; $BST204_{200}$, tumor-bearing mice treated with 5-fluorouracil and 200 mg/kg of BST204; MRI, magnetic resonance imaging; p.o. oral administration; i.p., intraperitoneal administration; H&E, hematoxylin and eosin staining; ELISA, enzyme-linked immunosorbent assay; LC-MS/MS, liquid chromatography with tandem mass spectrometry.

Figure 2

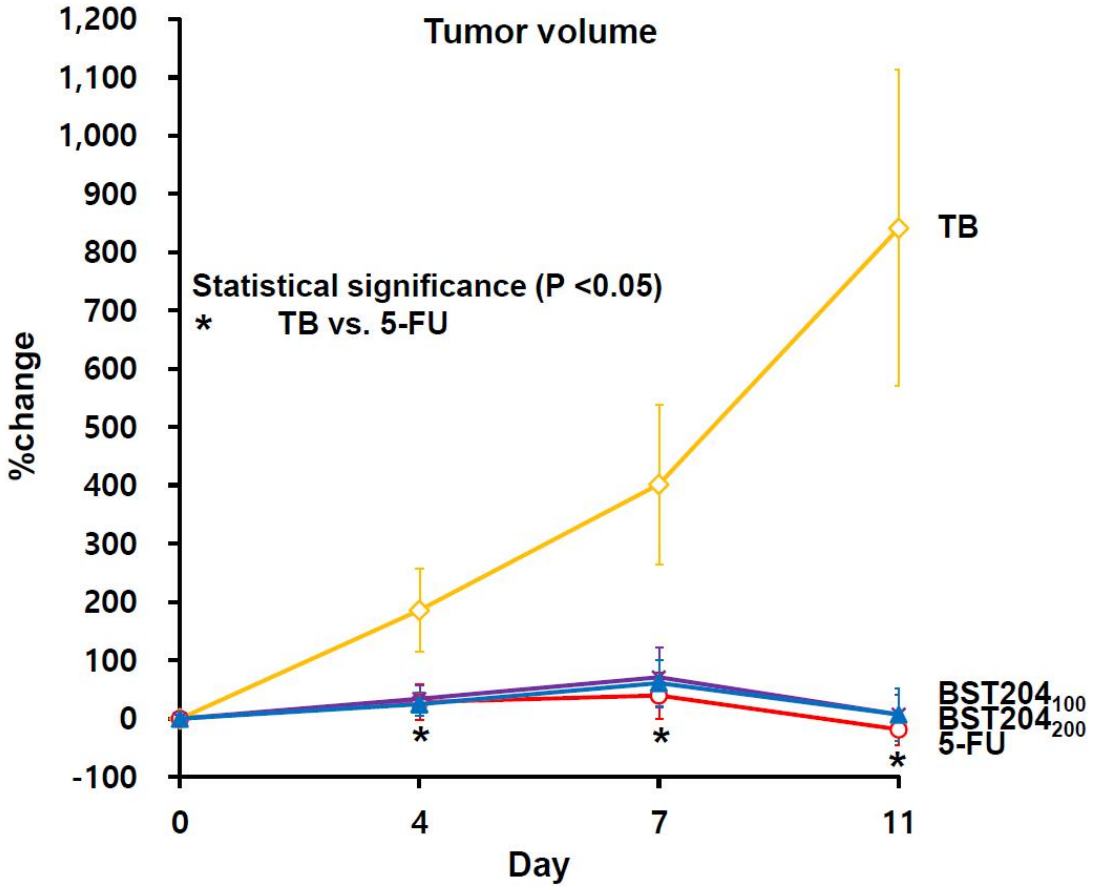

Figure 2. Percentage change in tumor growth.

The tumor volume was significantly decreased by 5-FU treatment. BST204 did not have a tumor inhibitory effect, as BST204-treated groups had a similar tumor volume compared with 5-FU group ($P > 0.05$). TB, untreated, tumor-bearing mice; 5-FU, tumor-bearing mice treated with 5-fluorouracil; $BST204_{100}$, tumor-bearing mice treated with 5-fluorouracil and 100 mg/kg of BST204; $BST204_{200}$, tumor-bearing mice treated with 5-fluorouracil and 200 mg/kg of BST204.

Figure 3

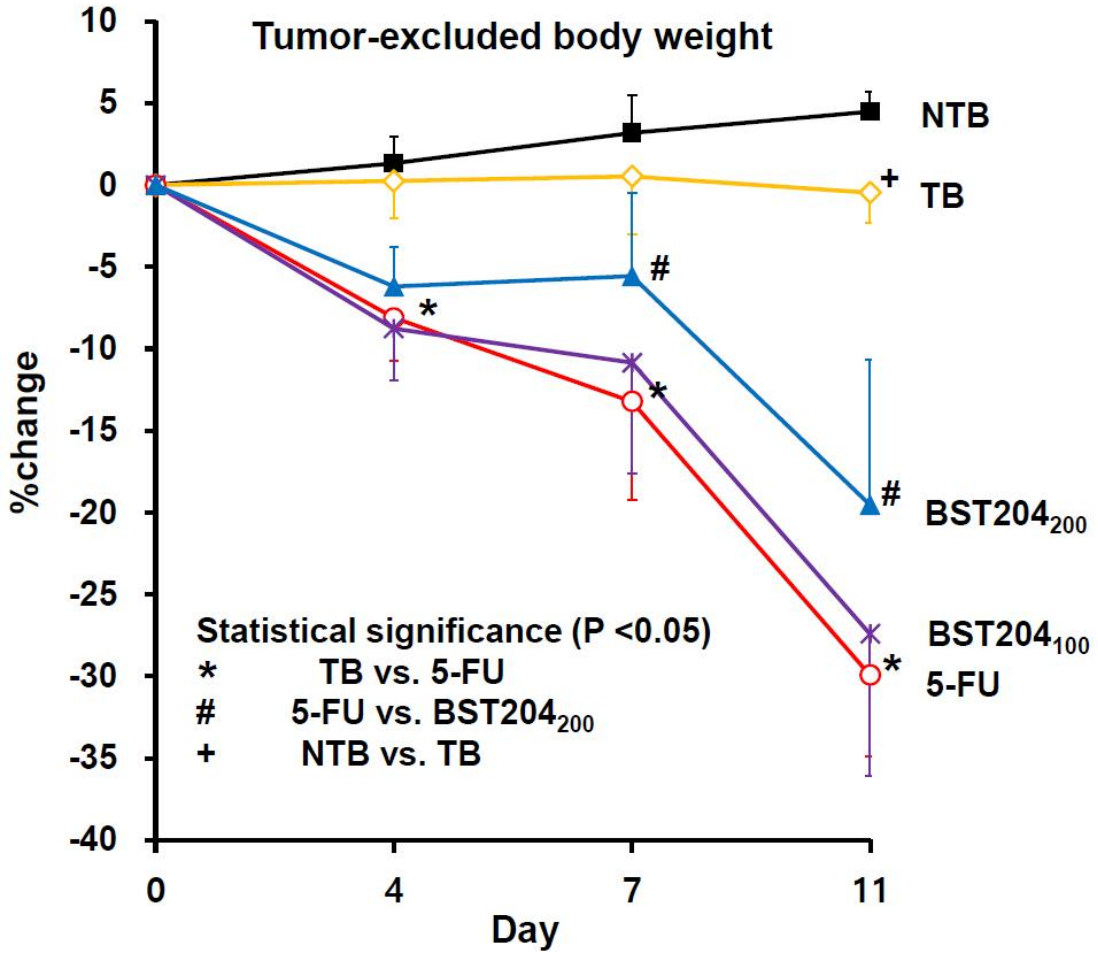

Figure 3. Changes in tumor-excluded body weight.

Chemotherapy with 5-FU caused significant cachexia (up to -30% tumor-excluded body weight change). This effect was significantly reduced in $BST204_{200}$ group. NTB group presented a significantly greater tumor-excluded body weight than TB group on day 11. The tumor-excluded body weight was measured in 10 mice from each group. NTB, untreated, non-tumor-bearing mice; TB, untreated, tumor-bearing mice; 5-FU, tumor-bearing mice treated with 5-fluorouracil; $BST204_{100}$, tumor-bearing mice treated with 5-fluorouracil and 100 mg/kg of BST204; $BST204_{200}$, tumor-bearing mice treated with 5-fluorouracil and 200 mg/kg of BST204.

Figure 4

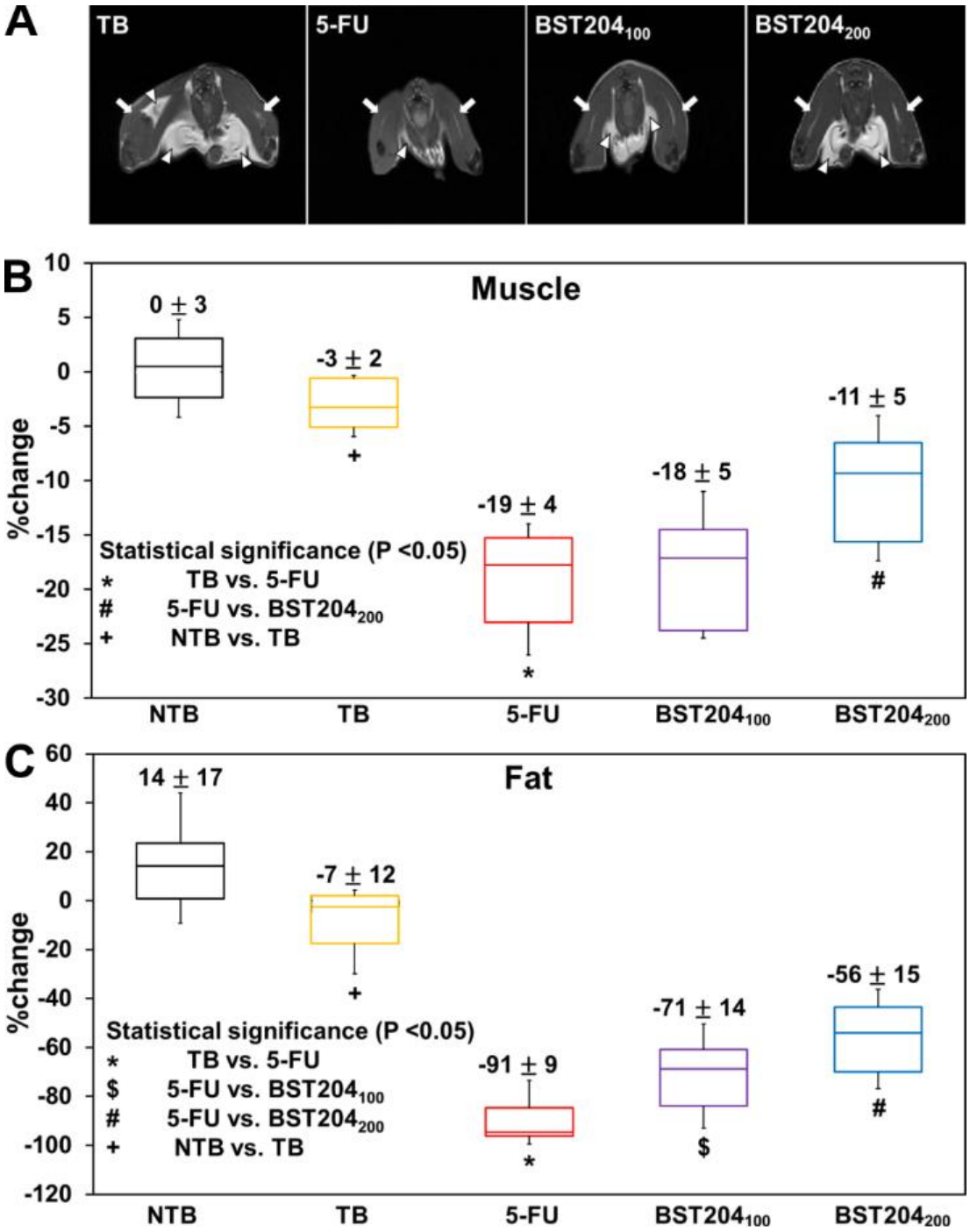
A
TB
5-FU
BST204100
BST204200
B
Muscle
%change
0 ± 3
-3 ± 2
-19 ± 4
-18 ± 5
-11 ± 5
Statistical significance (P <0.05)
* TB vs. 5-FU
# 5-FU vs. BST204200
+ NTB vs. TB
NTB
TB
5-FU
BST204100
BST204200
C
Fat
%change
14 ± 17
-7 ± 12
-91 ± 9
-71 ± 14
-56 ± 15
Statistical significance (P <0.05)
* TB vs. 5-FU
$ 5-FU vs. BST204100
# 5-FU vs. BST204200
+ NTB vs. TB
NTB
TB
5-FU
BST204100
BST204200

Figure 4. Change in muscle and fat volumes as observed using magnetic resonance imaging (MRI).

(A) MRIs revealed the considerable loss of muscle (arrows) and fat (arrowheads) in 5-FU group. Changes in muscle (B) and fat (C) contents. Muscle and fat volumes were analyzed in 10 mice from each group. NTB, untreated, non-tumor-bearing mice; TB, untreated, tumor-bearing mice; 5-FU, tumor-bearing mice treated with 5-fluorouracil; $BST204_{100}$, tumor-bearing mice treated with 5-fluorouracil and 100 mg/kg of BST204; $BST204_{200}$, tumor-bearing mice treated with 5-fluorouracil and 200 mg/kg of BST204.

Figure 5

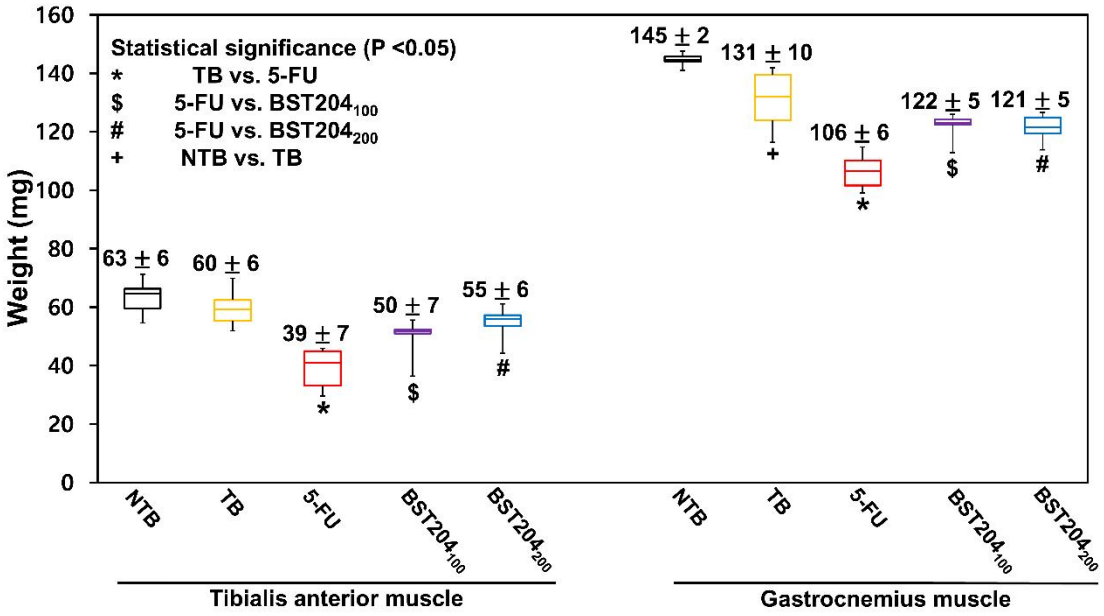

Figure 5. Intergroup comparisons of the tibialis anterior and gastrocnemius muscle weights.

Chemotherapy-induced cachexia was observed in 5-FU group, whereas BST204 treatment significantly alleviated chemotherapy-induced muscle atrophy. Data are presented as means ± standard deviations (n = 6 per group). NTB, untreated, non-tumor-bearing mice; TB, untreated, tumor-bearing mice; 5-FU, tumor-bearing mice treated with 5-fluorouracil; $BST204_{100}$, tumor-bearing mice treated with 5-fluorouracil and 100 mg/kg of BST204; $BST204_{200}$, tumor-bearing mice treated with 5-fluorouracil and 200 mg/kg of BST204.

Figure 6

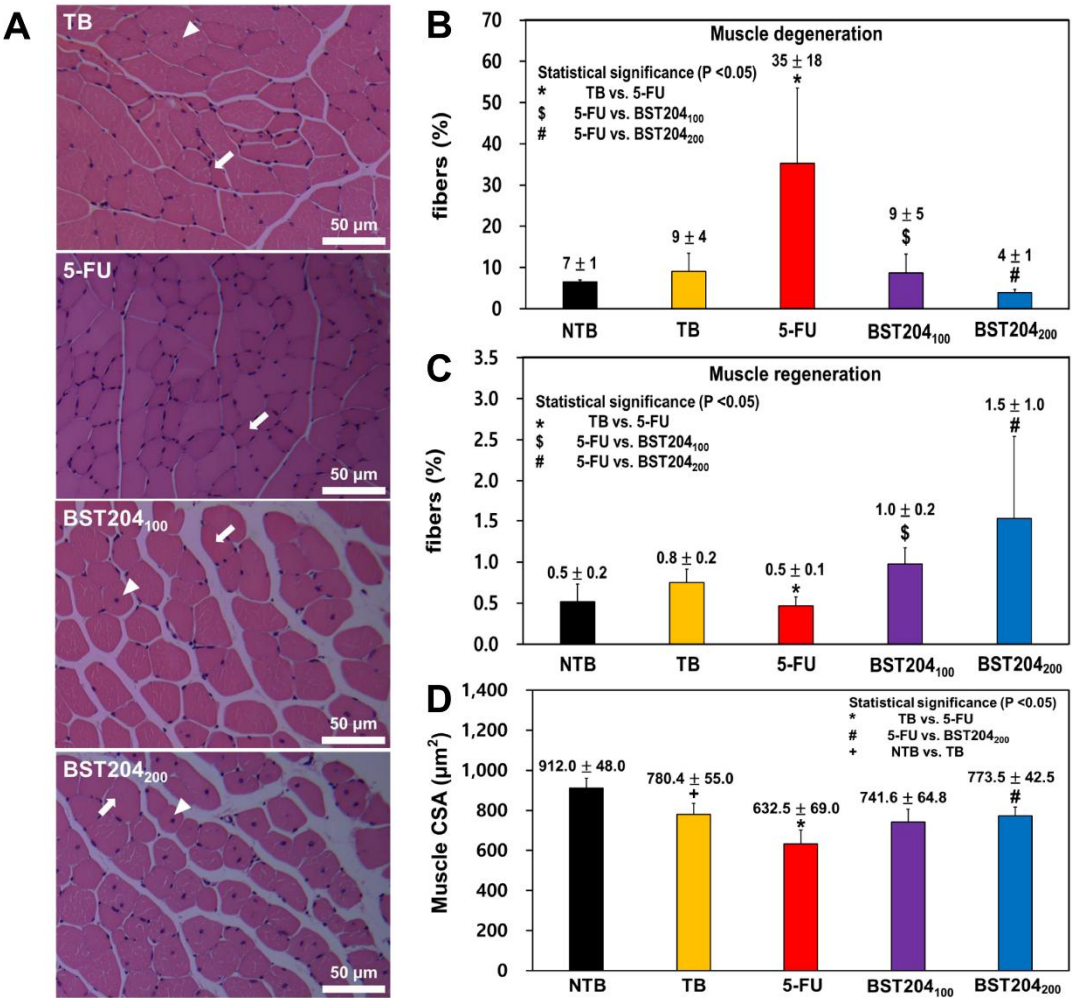

Figure 6. Histological examination of the anti-cachexic effect of BST204.

(A) H&E staining of the tibialis anterior muscle (×200) revealed an increased number of hyalinized and hypereosinophilic fibers (arrows) and a decreased number of fibers with central nuclei (arrowheads) in 5-FU group. Activities of muscle degeneration (B) and regeneration (C) were examined in 6 mice from each group. (D) Muscle CSA analyzed in 3 mice from each group. NTB, untreated, non-tumor-bearing mice; TB, untreated, tumor-bearing mice; 5-FU, tumor-bearing mice treated with 5-fluorouracil; $BST204_{100}$, tumor-bearing mice treated with 5-fluorouracil and 100 mg/kg of BST204; $BST204_{200}$, tumor-bearing mice treated with 5-fluorouracil and 200 mg/kg of BST204; CSA, cross-sectional area.

Figure 7

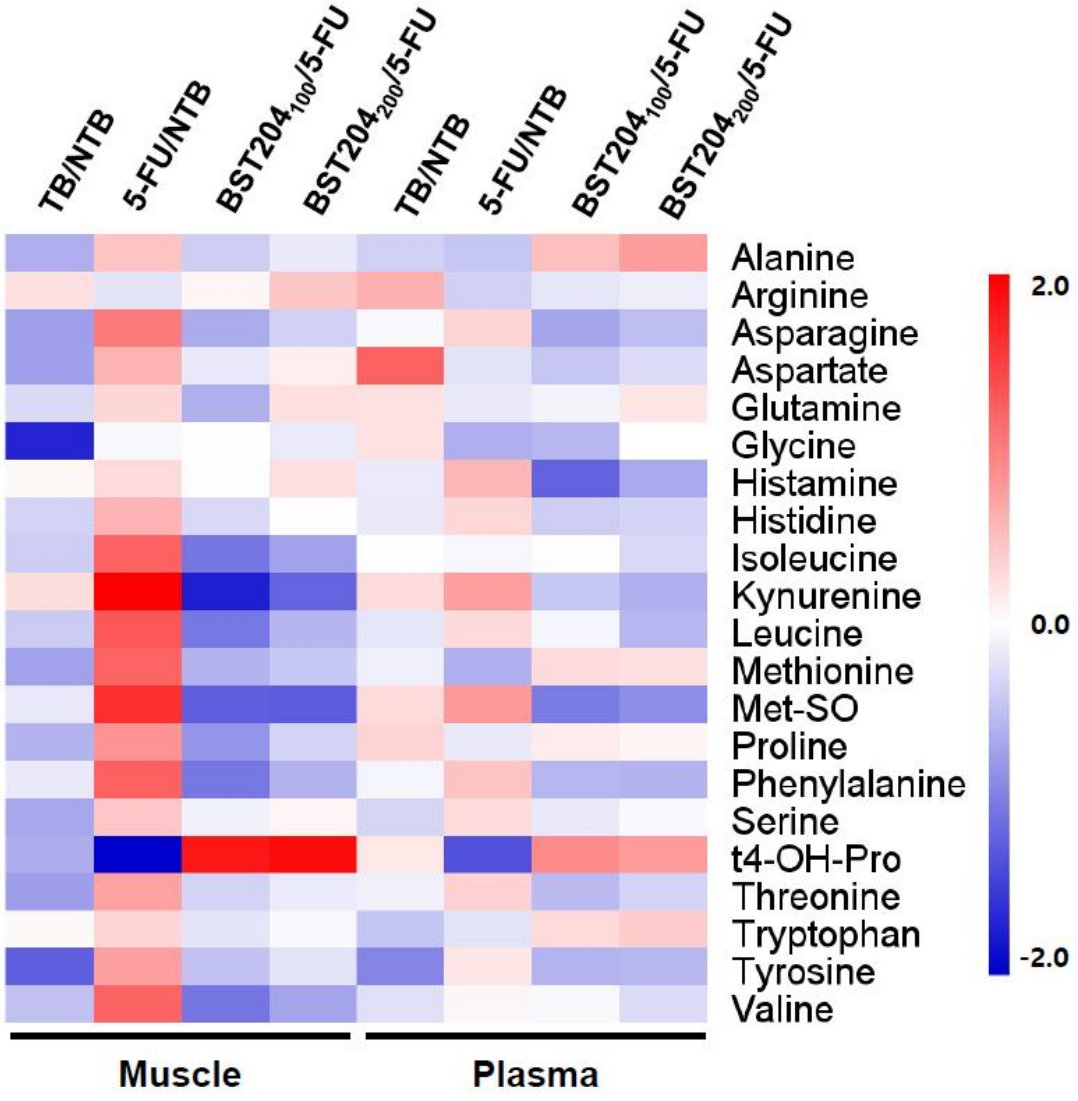

Figure 7. Heatmap for comparing 21 amino acids metabolites between groups.

Amino acid metabolites were evaluated in 6 mice from each group. NTB, untreated, non-tumor-bearing mice; TB, untreated, tumor-bearing mice; 5-FU, tumor-bearing mice treated with 5-fluorouracil; $BST204_{100}$, tumor-bearing mice treated with 5-fluorouracil and 100 mg/kg of BST204; $BST204_{200}$, tumor-bearing mice treated with 5-fluorouracil and 200 mg/kg of BST204; Met-SO, methionine sulfoxide; t4-OH-Pro, 4-hydroxyproline.

Figure 8

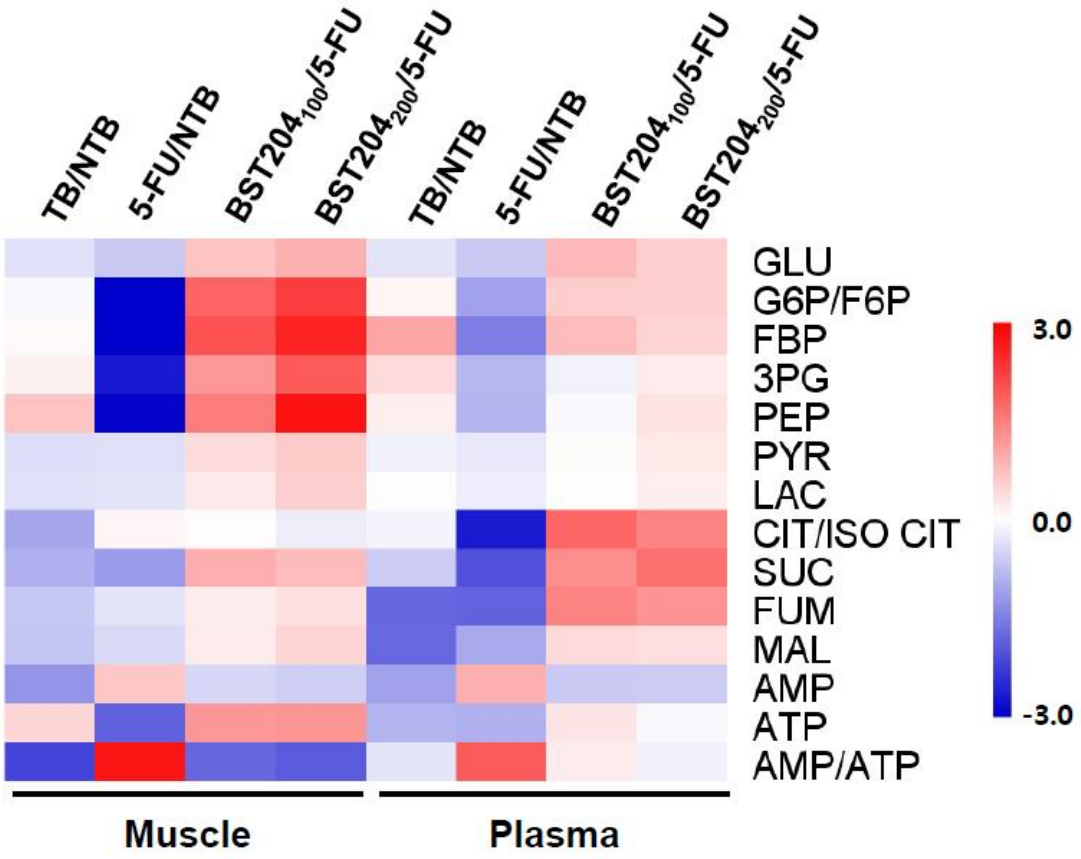

Figure 8. Heatmap for intergroup comparison of glucose, glycolysis intermediates, and TCA cycle metabolites.

The concentrations of glucose and metabolites in glycolysis and TCA cycle were analyzed in 6 mice from each group. NTB, untreated, non-tumor-bearing mice; TB, untreated, tumor-bearing mice; 5-FU, tumor-bearing mice treated with 5-fluorouracil; $BST204_{100}$, tumor-bearing mice treated with 5-fluorouracil and 100 mg/kg of BST204; $BST204_{200}$, tumor-bearing mice treated with 5-fluorouracil and 200 mg/kg of BST204; GLU, glucose; G6P/F6P, glucose-6-phosphate/fructose-6-phosphate; FBP, Fructose-1,6-bisphosphate; 3PG, 3-phosphoglycerate; PEP, Phosphoenolpyruvate; PYR, Pyruvate; LAC, Lactate; CIT/ISO CIT, Citrate/Iso citrate; SUC, Succinate; FUM, Fumarate; MAL, Malate; AMP, Adenosine monophosphate; ATP, Adenosine triphosphate; TCA cycle, tricarboxylic acid cycle.

Figure 9

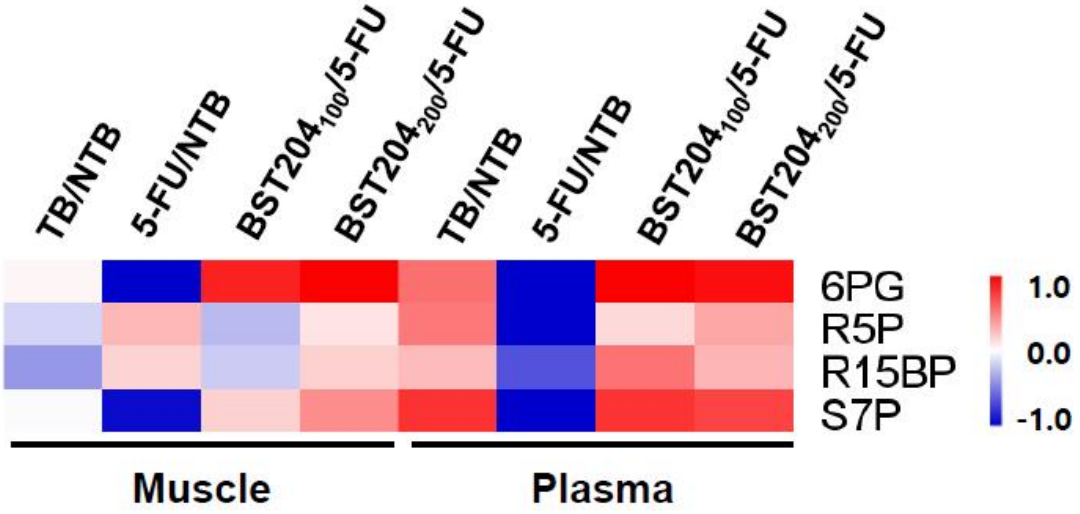

Figure 9. Heatmap for intergroup comparison of pentose phosphate pathway metabolites.

The concentrations of pentose phosphate pathway metabolites were analyzed in 6 mice from each group. NTB, untreated, non-tumor-bearing mice; TB, untreated, tumor-bearing mice; 5-FU, tumor-bearing mice treated with 5-fluorouracil; $BST204_{100}$, tumor-bearing mice treated with 5-fluorouracil and 100 mg/kg of BST204; $BST204_{200}$, tumor-bearing mice treated with 5-fluorouracil and 200 mg/kg of BST204; 6PG, 6-phosphogluconate; R5P, Ribulose-5-phosphate; R15BP, Ribose-1,5-bisphosphate; S7P, Sedoheptulose-7-phosphate.

Figure 10

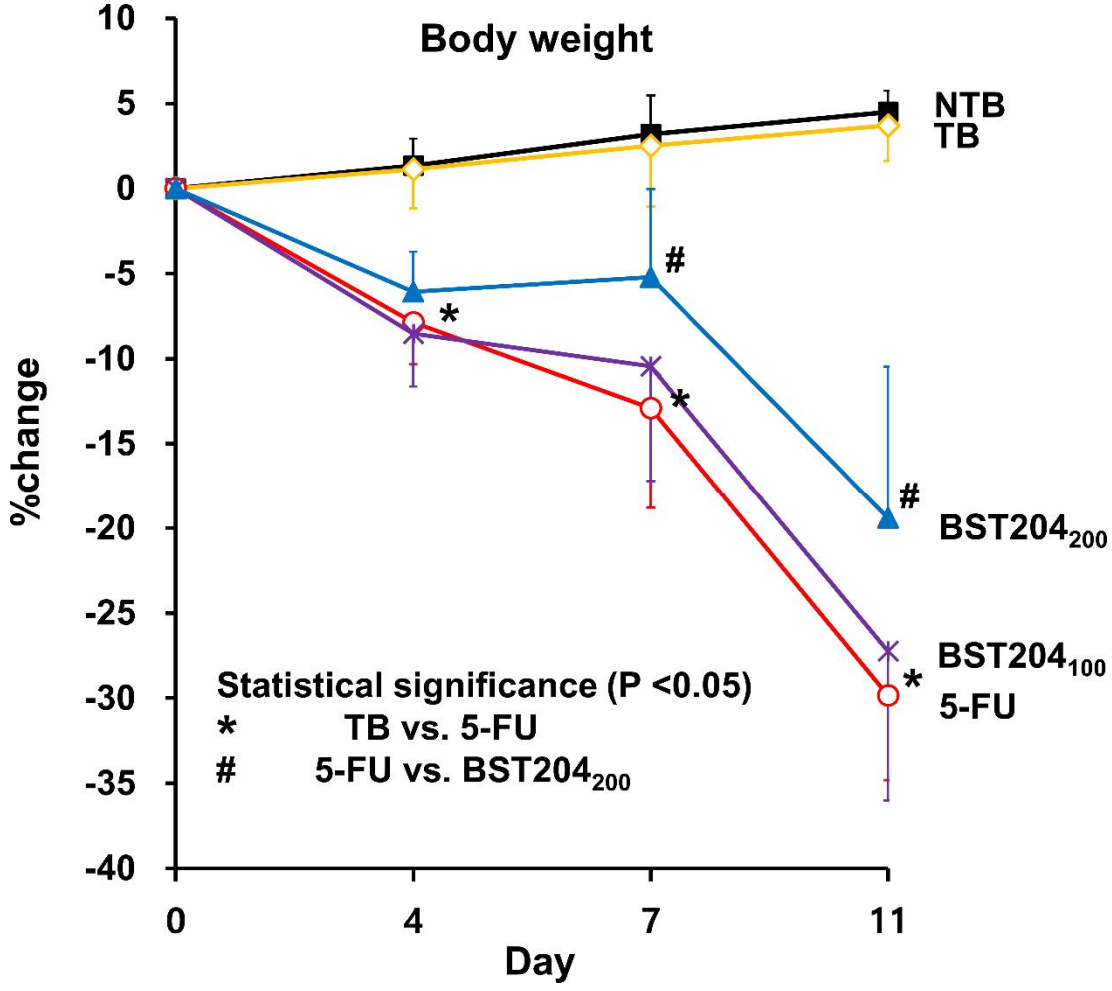

Figure 10. Percentage change in total body weight. There was no significant difference in the total body weight in TB group compared with that in NTB group ($P > 0.05$). NTB, untreated, non-tumor-bearing mice; TB, untreated, tumor-bearing mice; 5-FU, tumor-bearing mice treated with 5-fluorouracil; $BST204_{100}$, tumor-bearing mice treated with 5-fluorouracil and 100 mg/kg of BST204; $BST204_{200}$, tumor-bearing mice treated with 5-fluorouracil and 200 mg/kg of BST204.

REFERENCE

1. Barreto R, Waning DL, Gao H, Liu Y, Zimmers TA, Bonetto A. Chemotherapy-related cachexia is associated with mitochondrial depletion and the activation of ERK1/2 and p38 MAPKs. Oncotarget. 2016;7(28):43442-60. doi: 10.18632/oncotarget.9779. PubMed PMID: PMC5190036.

2. Aoyagi T, Terracina KP, Raza A, Matsubara H, Takabe K. Cancer cachexia, mechanism and treatment. World J Gastrointest Oncol. 2015;7(4):17-29. Epub 2015/04/22. doi: 10.4251/wjgo.v7.i4.17. PubMed PMID: 25897346; PubMed Central PMCID: PMCPMC4398892.

3. Yennurajalingam S, Tannir NM, Williams JL, Lu Z, Hess KR, Frisbee-Hume S, et al. A Double-Blind, Randomized, Placebo-Controlled Trial of Panax Ginseng for Cancer-Related Fatigue in Patients With Advanced Cancer. Journal of the National Comprehensive Cancer Network : JNCCN. 2017;15(9):1111-20. Epub 2017/09/07. doi: 10.6004/jnccn.2017.0149. PubMed PMID: 28874596.

4. Park HJ, Shim HS, Kim JY, Kim JY, Park SK, Shim I. Ginseng Purified Dry Extract, BST204, Improved Cancer Chemotherapy-Related Fatigue and Toxicity in Mice. Evidence-based complementary and alternative medicine : eCAM. 2015;2015:197459. Epub 2015/05/07. doi: 10.1155/2015/197459. PubMed PMID: 25945105; PubMed Central PMCID: PMCPMC4405287.

5. Seo JY, Lee JH, Kim NW, Kim YJ, Chang SH, Ko NY, et al. Inhibitory effects of a fermented ginseng extract, BST204, on the expression of inducible nitric oxide synthase and nitric oxide production in lipopolysaccharide-activated murine macrophages. J Pharm Pharmacol. 2005;57(7):911-8. Epub 2005/06/23. doi: 10.1211/0022357056497. PubMed PMID: 15969952.

6. Fu W, Xu H, Yu X, Lyu C, Tian Y, Guo M, et al. 20 (S)-Ginsenoside Rg2 attenuates myocardial ischemia/reperfusion injury by reducing oxidative stress and inflammation: Role of SIRT1. 2018;8(42):23947-62.

7. Xiao N, Yang LL, Yang YL, Liu LW, Li J, Liu B, et al. Ginsenoside Rg5 Inhibits Su

ccinate-Associated Lipolysis in Adipose Tissue and Prevents Muscle Insulin Resistance. Fron tiers in pharmacology. 2017;8:43. Epub 2017/03/07. doi: 10.3389/fphar.2017.00043. PubMed PMID: 28261091; PubMed Central PMCID: PMCPMC5306250.

8. Li W, Yan MH, Liu Y, Liu Z, Wang Z, Chen C, et al. Ginsenoside Rg5 Ameliorates Cisplatin-Induced Nephrotoxicity in Mice through Inhibition of Inflammation, Oxidative Stre ss, and Apoptosis. Nutrients. 2016;8(9). Epub 2016/09/21. doi: 10.3390/nu8090566. PubMed PMID: 27649238; PubMed Central PMCID: PMCPMC5037551.

9. Lee SM. Anti-inflammatory effects of ginsenosides Rg5 , Rz1 , and Rk1 : inhibition of TNF-alpha-induced NF-kappaB, COX-2, and iNOS transcriptional expression. Phytothera py research : PTR. 2014;28(12):1893-6. Epub 2014/07/22. doi: 10.1002/ptr.5203. PubMed P MID: 25042112.

10. Jourdain M, Melly S, Summermatter S, Hatakeyama S. Mouse models of cancer-in duced cachexia: Hind limb muscle mass and evoked force as readouts. Biochem Biophys Res Commun. 2018;503(4):2415-20. Epub 2018/07/04. doi: 10.1016/j.bbrc.2018.06.170. PubMe d PMID: 29969629.

11. Benson AB, 3rd, Venook AP, Cederquist L, Chan E, Chen YJ, Cooper HS, et al. Col on Cancer, Version 1.2017, NCCN Clinical Practice Guidelines in Oncology. Journal of the N ational Comprehensive Cancer Network : JNCCN. 2017;15(3):370-98. Epub 2017/03/10. Pu bMed PMID: 28275037.

12. Qi F, Zheng Z, Yan Q, Liu J, Chen Y, Zhang G. Comparisons of Efficacy, Safety, an d Cost of Chemotherapy Regimens FOLFOX4 and FOLFIRINOX in Rectal Cancer: A Rand omized, Multicenter Study. Medical science monitor : international medical journal of experi mental and clinical research. 2018;24:1970-9. Epub 2018/04/04. PubMed PMID: 29614063; PubMed Central PMCID: PMCPMC5896363.

13. Tisdale MJ, Dhesi JK. Inhibition of weight loss by omega-3 fatty acids in an experi mental cachexia model. Cancer research. 1990;50(16):5022-6. Epub 1990/08/15. PubMed P MID: 2379167.

14. Tanaka Y, Eda H, Fujimoto K, Tanaka T, Ishikawa T, Ishitsuka H. Anticachectic act ivity of 5'-deoxy-5-fluorouridine in a murine tumor cachexia model, colon 26 adenocarcinom

a. Cancer research. 1990;50(15):4528-32. Epub 1990/08/01. PubMed PMID: 1695121.

15. Le Bricon T, Gugins S, Cynober L, Baracos VE. Negative impact of cancer chemot herapy on protein metabolism in healthy and tumor-bearing rats. Metabolism: clinical and ex perimental. 1995;44(10):1340-8. Epub 1995/10/01. PubMed PMID: 7476295.

16. Xu Q, Brabham JG, Zhang S, Munster P, Fields K, Zhao RJ, et al. Chinese herbal f ormula, Bing De Ling, enhances antitumor effects and ameliorates weight loss induced by 5-f luorouracil in the mouse CT26 tumor model. DNA and cell biology. 2005;24(7):470-5. Epub 2005/07/13. doi: 10.1089/dna.2005.24.470. PubMed PMID: 16008516.

17. Barreto R, Mandili G, Witzmann FA, Novelli F, Zimmers TA, Bonetto A. Cancer an d Chemotherapy Contribute to Muscle Loss by Activating Common Signaling Pathways. Fro ntiers in physiology. 2016;7:472. Epub 2016/11/04. doi: 10.3389/fphys.2016.00472. PubMed PMID: 27807421; PubMed Central PMCID: PMCPMC5070123.

18. Pritt ML, Hall DG, Recknor J, Credille KM, Brown DD, Yumibe NP, et al. Fabp3 a s a biomarker of skeletal muscle toxicity in the rat: comparison with conventional biomarker s. Toxicological sciences : an official journal of the Society of Toxicology. 2008;103(2):382-96. Epub 2008/03/01. doi: 10.1093/toxsci/kfn042. PubMed PMID: 18308699.

19. Radaelli G, Piccirillo A, Birolo M, Bertotto D, Gratta F, Ballarin C, et al. Effect of a ge on the occurrence of muscle fiber degeneration associated with myopathies in broiler chic kens submitted to feed restriction. Poultry science. 2017;96(2):309-19. Epub 2016/08/28. doi: 10.3382/ps/pew270. PubMed PMID: 27566729.

20. Stewart MD, Lopez S, Nagandla H, Soibam B, Benham A, Nguyen J, et al. Mouse myofibers lacking the SMYD1 methyltransferase are susceptible to atrophy, internalization o f nuclei and myofibrillar disarray. Disease models & mechanisms. 2016;9(3):347-59. Epub 2 016/03/05. doi: 10.1242/dmm.022491. PubMed PMID: 26935107; PubMed Central PMCID: PMCPMC4833328.

21. Branco A, Yoshikawa FSY, Pietrobon AJ, Sato MN. Role of Histamine in Modulati ng the Immune Response and Inflammation. Mediators of inflammation. 2018;2018:952407 5. Epub 2018/09/19. doi: 10.1155/2018/9524075. PubMed PMID: 30224900; PubMed Centr al PMCID: PMCPMC6129797.

22. Wang Q, Liu D, Song P, Zou MH. Tryptophan-kynurenine pathway is dysregulated in inflammation, and immune activation. Frontiers in bioscience (Landmark edition). 2015;20:1116-43. Epub 2015/05/12. PubMed PMID: 25961549; PubMed Central PMCID: PMCPMC4911177.

23. Allu PK, Marada A, Boggula Y, Karri S, Krishnamoorthy T, Sepuri NB. Methionine sulfoxide reductase 2 reversibly regulates Mge1, a cochaperone of mitochondrial Hsp70, during oxidative stress. Molecular biology of the cell. 2015;26(3):406-19. Epub 2014/11/28. doi: 10.1091/mbc.E14-09-1371. PubMed PMID: 25428986; PubMed Central PMCID: PMCPMC4310733.

24. Kumar Srivastava A, Khare P, Kumar Nagar H, Raghuwanshi N, Srivastava R. Hydroxyproline: A Potential Biochemical Marker and Its Role in the Pathogenesis of Different Diseases. Current Protein & Peptide Science. 2016;17(6):596-602. doi: 10.2174/1389203717666151201192247.

25. Stincone A, Prigione A, Cramer T, Wamelink MM, Campbell K, Cheung E, et al. The return of metabolism: biochemistry and physiology of the pentose phosphate pathway. Biological reviews of the Cambridge Philosophical Society. 2015;90(3):927-63. Epub 2014/09/23. doi: 10.1111/brv.12140. PubMed PMID: 25243985; PubMed Central PMCID: PMCPMC4470864.

26. Parasuraman S, Raveendran R, Kesavan R. Blood sample collection in small laboratory animals. Journal of pharmacology & pharmacotherapeutics. 2010;1(2):87-93. Epub 2011/02/26. doi: 10.4103/0976-500x.72350. PubMed PMID: 21350616; PubMed Central PMCID: PMCPMC3043327.

27. da Silva CG, Jarzyna R, Specht A, Kaczmarek E. Extracellular nucleotides and adenosine independently activate AMP-activated protein kinase in endothelial cells: involvement of P2 receptors and adenosine transporters. Circulation research. 2006;98(5):e39-47. Epub 2006/02/25. doi: 10.1161/01.RES.0000215436.92414.1d. PubMed PMID: 16497986; PubMed Central PMCID: PMCPMC2830086.

28. Seo JY, Lee JH, Kim NW, Her E, Chang SH, Ko NY, et al. Effect of a fermented ginseng extract, BST204, on the expression of cyclooxygenase-2 in murine macrophages. Int I

mmunopharmacol. 2005;5(5):929-36. Epub 2005/03/22. doi: 10.1016/j.intimp.2005.01.008. PubMed PMID: 15778128.

29. Hofseth LJ, Wargovich MJ. Inflammation, Cancer, and Targets of Ginseng. The Jou rnal of Nutrition. 2007;137(1):183S-5S. doi: 10.1093/jn/137.1.183S.

30. Park MW, Ha J, Chung SH. 20(S)-ginsenoside Rg3 enhances glucose-stimulated in sulin secretion and activates AMPK. Biological & pharmaceutical bulletin. 2008;31(4):748-5 1. Epub 2008/04/02. PubMed PMID: 18379076.

31. Shen L, Haas M, Wang DQH, May A, Lo CC, Obici S, et al. Ginsenoside Rb1 incre ases insulin sensitivity by activating AMP-activated protein kinase in male rats. Physiologica l Reports. 2015;3(9):e12543. doi: 10.14814/phy2.12543. PubMed PMID: PMC4600387.

32. Pin F, Barreto R, Couch ME, Bonetto A, O'Connell TM. Cachexia induced by canc er and chemotherapy yield distinct perturbations to energy metabolism. Journal of cachexia, s arcopenia and muscle. 2019;10(1):140-54. Epub 2019/01/27. doi: 10.1002/jcsm.12360. Pub Med PMID: 30680954; PubMed Central PMCID: PMCPMC6438345.

33. Schiaffino S, Dyar KA, Ciciliot S, Blaauw B, Sandri M. Mechanisms regulating sk eletal muscle growth and atrophy. The FEBS journal. 2013;280(17):4294-314. Epub 2013/03 /23. doi: 10.1111/febs.12253. PubMed PMID: 23517348.

34. Ballarò R, Penna F, Pin F, Gómez-Cabrera MC, Viña J, Costelli P. Moderate Exerci se Improves Experimental Cancer Cachexia by Modulating the Redox Homeostasis. Cancers. 2019;11(3). Epub 2019/03/03. doi: 10.3390/cancers11030285. PubMed PMID: 30823492; P ubMed Central PMCID: PMCPMC6468783.

35. Braun TP, Szumowski M, Levasseur PR, Grossberg AJ, Zhu X, Agarwal A, et al. M uscle atrophy in response to cytotoxic chemotherapy is dependent on intact glucocorticoid si gnaling in skeletal muscle. PloS one. 2014;9(9):e106489. Epub 2014/09/26. doi: 10.1371/jou rnal.pone.0106489. PubMed PMID: 25254959; PubMed Central PMCID: PMCPMC417781 5.

36. Aquila G, Re Cecconi AD, Brault JJ, Corli O, Piccirillo R. Nutraceuticals and Exer cise against Muscle Wasting during Cancer Cachexia. Cells. 2020;9(12). Epub 2020/12/02. d oi: 10.3390/cells9122536. PubMed PMID: 33255345; PubMed Central PMCID: PMCPMC7

760926.

37. Rittig N, Bach E, Thomsen HH, Pedersen SB, Nielsen TS, Jørgensen JO, et al. Regulation of Lipolysis and Adipose Tissue Signaling during Acute Endotoxin-Induced Inflammation: A Human Randomized Crossover Trial. PloS one. 2016;11(9):e0162167-e. doi: 10.1371/journal.pone.0162167. PubMed PMID: 27627109.

38. Le Lay S, Simard G, Martinez MC, Andriantsitohaina R. Oxidative stress and metabolic pathologies: from an adipocentric point of view. Oxidative medicine and cellular longevity. 2014;2014:908539. Epub 2014/08/22. doi: 10.1155/2014/908539. PubMed PMID: 25143800; PubMed Central PMCID: PMCPMC4131099.

39. Luo L, Liu M. Adipose tissue in control of metabolism. The Journal of endocrinology. 2016;231(3):R77-r99. Epub 2016/12/10. doi: 10.1530/joe-16-0211. PubMed PMID: 27935822.

40. Quan-Jun Y, Yan H, Yong-Long H, Li-Li W, Jie L, Jin-Lu H, et al. Selumetinib Attenuates Skeletal Muscle Wasting in Murine Cachexia Model through ERK Inhibition and AKT Activation. Molecular cancer therapeutics. 2017;16(2):334-43. Epub 2016/09/08. doi: 10.1158/1535-7163.Mct-16-0324. PubMed PMID: 27599525.

41. Lin XY, Chen SZ. Calpain inhibitors ameliorate muscle wasting in a cachectic mouse model bearing CT26 colorectal adenocarcinoma. Oncology reports. 2017;37(3):1601-10. Epub 2017/01/24. doi: 10.3892/or.2017.5396. PubMed PMID: 28112357.

42. Musarò A. The Basis of Muscle Regeneration. Advances in Biology. 2014;2014:612471. doi: 10.1155/2014/612471.

43. Bonetto A, Aydogdu T, Jin X, Zhang Z, Zhan R, Puzis L, et al. JAK/STAT3 pathway inhibition blocks skeletal muscle wasting downstream of IL-6 and in experimental cancer cachexia. American journal of physiology Endocrinology and metabolism. 2012;303(3):E410-21. Epub 2012/06/07. doi: 10.1152/ajpendo.00039.2012. PubMed PMID: 22669242; PubMed Central PMCID: PMCPMC3423125.

44. Eskiler GG, Bezdegumeli E, Ozman Z, Ozkan AD, Bilir C, Kucukakca BN, et al. IL-6 mediated JAK/STAT3 signaling pathway in cancer patients with cachexia. Bratislavske lekarske listy. 2019;66(11):819-26. Epub 2019/11/22. doi: 10.4149/bll_2019_136. PubMed P

MID: 31747761.

45. Niu M, Song S, Su Z, Wei L, Li L, Pu W, et al. Inhibition of HSP90 reversed STAT 3 mediated muscle wasting induced by cancer cachexia. 2021:2021.01.27.428420. doi: 10.11 01/2021.01.27.428420 %J bioRxiv.

국문요약

악액질의 새로운 치료 전략 개발을 위한 항암 화학 요법에 의해 유도된 악액질 마우스 모델에서 BST204 의 치료 효과에 관한 연구

암 악액질 (cancer cachexia)은 암에 의한 신체의 비정상적 대사 기능으로 인하여 체중과 근육 등이 지속적으로 소실되는 상태로 암 환자의 삶의 질 및 항암 치료 효과의 저하를 초래한다. 암을 치료하기 위해 사용되는 항암 화학 요법 (chemotherapy) 또한 암 악액질의 주요 원인 중 하나로 알려져 있어 효과적인 항암 치료를 위해 항암 화학 요법으로 인한 악액질을 개선시킬 수 있는 치료 전략의 개발이 필요하다.

인삼 사포닌의 일종인 진세노사이드 (ginsenosides)는 염증 (inflammation) 및 산화적 스트레스 (oxidative stress)의 억제 그리고 에너지 생산 촉진과 같은 다양한 건강 증진 효과를 가지고 있다. BST204 는 여러 종류의 진세노사이드 중 특히 Rh2 와 Rg3 의 함량이 증진된 인삼 정제 건조 추출물로써 항암 화학 요법과 관련된 피로와 독성을 줄일 수 있는 가능성을 보여주고 있다.

항암 화학 요법으로 유발된 악액질에서 BST204 의 악액질 개선 가능성을 확인하기 위하여, CT-26 세포주를 동종 이식한 대장암 마우스 모델에 항암제인 5- 플루오로유라실 (5-Fluorouracil, 5-FU)를 투여를 통해 항암 화학 요법으로 유도된 악액질 마우스 모델을 만들고 BST204 를 농도별로 투여하였다.

항암제로 인한 악액질 모델에서 BST204 의 투여는 종양을 제외한 체중 (5-FU 그룹 대 BST204 그룹의 변화: 7 일에 -13 % 대 -6 %, 11 일에 -30 % vs. -20 %), 근육량 (-19 % 대 -11 %) 그리고 지방량 (-91 % 대 -56 %)의 감소를 완화시켜주는 주는 효과를 보였다.

또한 조직학적으로 BST204 는 항암 화학 요법에 의한 근육의 재생과 퇴행 사이의 불균형을 개선시키고 근육 단면적 (cross-sectional area)의 감소를 완화시켰다.

대사체 분석을 통해 항암 화학 요법으로 유도 된 악액질은 염증, 산화적 스트레스 및 골격근의 분해를 활성화 시키고 골격근의 안정화 및 탄수화물 대사 (glycolysis, TCA cycle, and pentose phosphate pathway)의 활성을 감소시키는 특징을 보였다. 이러한 화학 항암 요법에 의한 악액질의 대사체적 특징들은 BST204 투여에 의해 유의미하게 개선됨을 확인할 수 있었다.

결론적으로, 이번 연구에서는 다각적 연구 방법을 통해 BST204 가 항암 화학 요법으로 인한 악액질을 효과적으로 완화시킬 수 있음을 보여주었다.